

See discussions, stats, and author profiles for this publication at: <https://www.researchgate.net/publication/23168493>

# Theoretical Study on Second Hyperpolarizabilities of Singlet Diradical Square Planar Nickel Complexes Involving o – Semiquinonato Type Ligands

ARTICLE in THE JOURNAL OF PHYSICAL CHEMISTRY A · OCTOBER 2008

Impact Factor: 2.69 · DOI: 10.1021/jp804400s · Source: PubMed

CITATIONS

37

READS

28

11 AUTHORS, INCLUDING:



Ryohei Kishi

Osaka University

110 PUBLICATIONS 1,947 CITATIONS

SEE PROFILE



Benoît Champagne

University of Namur

401 PUBLICATIONS 8,719 CITATIONS

SEE PROFILE



Edith Botek

Belgian Institute for Space Aeronomy

104 PUBLICATIONS 2,277 CITATIONS

SEE PROFILE



Masayoshi Nakano

Osaka University

337 PUBLICATIONS 4,769 CITATIONS

SEE PROFILE

# Theoretical Study on Second Hyperpolarizabilities of Singlet Diradical Square Planar Nickel Complexes Involving *o*-Semiquinonato Type Ligands

Hitoshi Fukui,<sup>†</sup> Ryohei Kishi,<sup>†</sup> Takuya Minami,<sup>†</sup> Hiroshi Nagai,<sup>†</sup> Hideaki Takahashi,<sup>†</sup> Takashi Kubo,<sup>‡</sup> Kenji Kamada,<sup>§</sup> Koji Ohta,<sup>§</sup> Benoît Champagne,<sup>||</sup> Edith Botek,<sup>||</sup> and Masayoshi Nakano<sup>\*,†</sup>

Department of Materials Engineering Science, Graduate School of Engineering Science, Osaka University, Toyonaka, Osaka 560-8531, Japan, Department of Chemistry, Graduate School of Science, Osaka University, Toyonaka, Osaka 560-0043, Japan, Photonics Research Institute, National Institute of Advanced Industrial Science and Technology (AIST), Ikeda, Osaka 563-8577, Japan, and Laboratoire de Chimie Théorique Appliquée, Facultés Universitaires Notre-Dame de la Paix (FUNDP), rue de Bruxelles, 61, B-5000 Namur, Belgium

Received: May 19, 2008; Revised Manuscript Received: June 29, 2008

Hybrid density functional theory method is applied for investigating the diradical character dependence of the second hyperpolarizability ( $\gamma$ ) of square planar nickel complexes involving several types of bidentate ligands [*o*-C<sub>6</sub>H<sub>4</sub>XY, where X = Y = O, NH, S, Se, and PH as well as (X, Y) = (NH, NH<sub>2</sub>) and (S, NH<sub>2</sub>)]. It is found that, as a function of the donor atoms, the diradical character of these complexes varies from 0.0 to 0.884 and is associated with substantial variations of  $\gamma$  ranging from  $14 \times 10^3$  to  $819 \times 10^3$  au. In particular, the largest  $\gamma$  values are associated with intermediate diradical characters in good agreement with the structure–property relationship obtained for pure hydrocarbon systems. Increasing the electronegativity of the X and Y donor groups of the ligands leads to larger diradical characters as a result of the enhancement of the double bond nature of the C=X(Y) bonds, which further stabilizes the diradicals on both-end benzene rings. This demonstrates that the electronegativities of the donor atoms of the ligands become a tuning parameter of the diradical character and then of the  $\gamma$  values of these complexes.

## 1. Introduction

For the past three decades, many kinds of organic compounds exhibiting highly efficient nonlinear optical (NLO) properties have been intensely studied owing to their potential applications in photonic devices such as optical switching, three-dimensional memory, optical limiting, and photodynamic therapy.<sup>1–3</sup> In particular, a great deal of attention has been paid to the third-order NLO properties, for example, two-photon absorption,<sup>4</sup> of organic  $\pi$ -conjugated compounds because of their large second hyperpolarizabilities ( $\gamma$ ), the microscopic origin of the third-order NLO properties, and the ultrafast response. The experimental and theoretical studies on these third-order NLO systems have revealed several tuning parameters of the amplitude and sign of  $\gamma$ , including the  $\pi$ -conjugation length, the bond length alternation, the strength of donor/acceptor substituents, and the charge,<sup>5–9</sup> but most of these studies have focused on closed-shell systems. Recently, we have investigated open-shell molecular systems as a novel class of NLO systems and, in particular, we have found that the singlet diradical systems with intermediate diradical character tend to exhibit a large enhancement of  $\gamma$  as compared to the parent closed-shell and pure diradical systems.<sup>10–12</sup> The mechanism governing the relationship between the diradical character and  $\gamma$  was theoretically clarified by adopting the valence configuration interaction (VCI) method using a two-site system.<sup>13</sup> This relationship has then

been verified by computational and experimental studies on several model and real organic molecular systems: the H<sub>2</sub> dissociation model,<sup>10b,e</sup> the twisted ethylene model,<sup>10a</sup> the diphenalenyl diradical systems,<sup>10d,11</sup> and the  $\pi$ -conjugated diradical systems involving imidazole rings.<sup>10c,14</sup>

On the other hand, transition-metal compounds are known to display diradical character.<sup>15,16</sup> In particular, recent theoretical and experimental studies have shown that square planar nickel complexes involving two bidentate ligands [Ni(*o*-C<sub>6</sub>H<sub>4</sub>XY)<sub>2</sub>] [where X = Y = O, NH, and S as well as (X, Y) = (NH, S) and (NH, O)] give different singlet diradical characters and that the amount of the diradical character is related to the stability of the semiquinone forms of the ligands depending on the strength of the double bond between the donor atom (X, Y) and the ring carbon.<sup>15</sup> Several experimental studies employing the degenerate four wave mixing (DFWM) technique have also shown that some of these complexes exhibit large  $\gamma$  values.<sup>17</sup> However, the latter systems have been considered to be closed-shell and have not so far been investigated from the viewpoint of their possible open-shell character. Indeed, the large  $\gamma$  values of these systems have been predicted to only originate from the extended  $\pi$ -delocalization over both-end rings through the core metal whereas the open-shell (diradical) character has recently turned out to be essential for the description of electronic structures of these complexes as mentioned above.

The present study, therefore, contributes to the elucidation of the origin of  $\gamma$  in these open-shell complexes. Namely, the diradical character dependence of  $\gamma$  in metal involving singlet diradical complexes [Ni(*o*-C<sub>6</sub>H<sub>4</sub>X<sub>2</sub>)<sub>2</sub>] is rationalized as a function of the donor atoms (X = O, NH, S, Se, and PH) by using the density functional theory and a hybrid exchange–correlation functional containing 50% of Hartree–Fock exchange, the

\* To whom correspondence should be addressed. Fax: +81-6-6850-6268. E-mail: mnaka@cheng.es.osaka-u.ac.jp.

<sup>†</sup> Department of Materials Engineering Science, Graduate School of Engineering Science, Osaka University.

<sup>‡</sup> Department of Chemistry, Graduate School of Science, Osaka University.

<sup>§</sup> National Institute of Advanced Industrial Science and Technology.

<sup>||</sup> Facultés Universitaires Notre-Dame de la Paix.

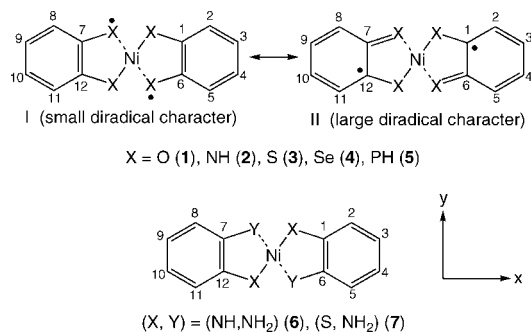


**Figure 1.** Resonance structures of singlet diradical square planar nickel complexes involving *o*-semiquinonate type ligands  $[\text{Ni}(\text{o-C}_6\text{H}_4\text{X}_2)_2]$ , where  $\text{X} = \text{O}$  (1),  $\text{NH}$  (2),  $\text{S}$  (3),  $\text{Se}$  (4), and  $\text{PH}$  (5). Reference closed-shell complexes  $[\text{Ni}(\text{o-C}_6\text{H}_4\text{XY})_2]$ , where  $(\text{X}, \text{Y}) = (\text{NH}, \text{NH}_2)$  (6) and  $(\text{S}, \text{NH}_2)$  (7), are also shown.

BHandHLYP functional. As reference systems, we examine two closed-shell nickel complexes  $[\text{Ni}(\text{o-C}_6\text{H}_4\text{XY})_2]$  [where  $(\text{X}, \text{Y}) = (\text{NH}, \text{NH}_2)$  and  $(\text{S}, \text{NH}_2)$ ]. On the basis of these results, we discuss the applicability of the structure–property relationships deduced from the results of pure organic diradical systems to these transition-metal complexes, and we propose a way of controlling the diradical character.

## 2. Theoretical and Computational Aspects

**2.1. Molecular Structures and Diradical Character.** Figure 1 shows the structures and coordinate axes of singlet diradical square planar nickel complexes involving *o*-semiquinonato type ligands  $[\text{Ni}(\text{o-C}_6\text{H}_4\text{X}_2)_2]$ , where  $\text{X} = \text{O}$  (1),  $\text{NH}$  (2),  $\text{S}$  (3),  $\text{Se}$  (4), and  $\text{PH}$  (5), and their reference closed-shell analogues  $[\text{Ni}(\text{o-C}_6\text{H}_4\text{XY})_2]$ , where  $(\text{X}, \text{Y}) = (\text{NH}, \text{NH}_2)$  (6) and  $(\text{S}, \text{NH}_2)$  (7). All complexes lie in the *xy* plane with their longitudinal axis along the *x*-direction. The structures of 1–5 (6–7) belong to the  $D_{2h}$  ( $C_{2h}$ ) point group in which the longitudinal axis is defined as a line passing through the midpoints between C3 and C4 and between C9 and C10 (Figure 1). From the possible resonance structures of 1–5 shown in Figure 1, the diradical character of structure II is predicted to be larger than that of structure I because of (1) the stabilization of the unpaired electrons through the delocalization in both-end phenyl rings in II and (2) the increase of singlet–triplet gap by superexchange interaction between two unpaired electrons on donor atoms X through Ni atom in I. It is expected that a modification of the donor atoms (X) in the ligands of  $[\text{Ni}(\text{o-C}_6\text{H}_4\text{X}_2)_2]$  will change the weights of I and II, which will lead to variations in the diradical character of these complexes.

Structures 1–2 were optimized at the spin-unrestricted B3LYP (UB3LYP) level of approximation since the B3LYP method is known to well reproduce the experimental structures of this type of conjugated diradical systems.<sup>18,19</sup> The geometry optimizations for 3–7 were performed using the spin-restricted B3LYP (RB3LYP) method because the symmetry broken solutions are not obtained using the UB3LYP method. For the fourth-row atoms, Ni and Se, we employed the SDD basis set developed by Bergner et al.,<sup>20,21</sup> while the 6–31G\* basis set was employed for the other atoms. The SDD basis set of Ni includes a pseudopotential representing Ne-like core and (8s7p6d1f)/[6s5p3d1f]-GTO valence basis set, whereas that for Se has a pseudopotential representing [Ar]3d<sup>10</sup>-like core and (4s5p)/[2s3p] valence basis set. This type of basis set combination was employed here owing to its reliability of reproducing the experimental geometries and of providing relative diradical characters of this kind of complexes.<sup>15,18</sup> So, the optimized

geometries of 1–3 (see Supporting Information) can be compared to the X-ray structures reported in ref 15 for systems that only differ by the presence of *t*-butyl substituents. In particular, the theory well reproduces the experimental trend describing an increase of diradical character from 3 to 1 with subsequent lengthening of the C1–C6 bond and shortening of the C1–X bond.

The diradical character was obtained from spin-unrestricted Hartree-Fock (UHF) calculations as follows. The diradical character  $y_i$  related to HOMO-*i* and LUMO+*i*, where HOMO and LUMO mean the highest-occupied and the lowest-occupied molecular orbitals, respectively, is defined by the weight of the doubly excited configuration in the multiconfigurational self-consistent field (MC-SCF) theory and is formally expressed in the spin-projected UHF (PUHF) theory as<sup>22,23</sup>

$$y_i = 1 - \frac{2T_i}{1 + T_i^2} \quad (1)$$

where  $T_i$  is the orbital overlap between the corresponding orbital pairs<sup>22,23</sup> ( $\chi_{\text{HOMO}-i}$  and  $\eta_{\text{HOMO}-i}$ ) and can also be represented using the occupation numbers ( $n_i$ ) of UHF natural orbitals (UNOs):

$$T_i = \frac{n_{\text{HOMO}-i} - n_{\text{LUMO}+i}}{2} \quad (2)$$

The diradical character  $y_i$  obtained from the UNO occupation numbers takes a value between 0 and 1, which correspond to the closed-shell and pure diradical systems, respectively. The present calculation scheme using the UNOs is the simplest, but it can well reproduce the diradical character calculated by other methods such as the *ab initio* configuration interaction (CI) method.<sup>24</sup> The present formula employs the UHF NOs and not the UDFT NOs, which would lead to incorrect lower diradical character in the present formula.

**2.2. Calculation and Analysis Methods of Static Second Hyperpolarizability.** It turns out from our previous studies<sup>10a,d,11</sup> that the UBHandHLYP method<sup>25</sup> well reproduces the  $\gamma$  values of diradical molecules with intermediate and large diradical characters calculated using the highly correlated UCCSD(T) methods, at least for systems, the size of which enables such comparison. Moreover, in these systems, the spin-polarized orbitals are dominantly located on both-end benzene rings as well as on the ligands and, as a consequence, the core metal orbitals only provide a marginal contribution to  $\gamma$ . We therefore employed the UBHandHLYP method to calculate  $\gamma_{xxxx}$  (hereafter referred to as  $\gamma$ ), the longitudinal tensor component, which dominates the third-order response and is sufficient for unraveling the relationship between the diradical character and  $\gamma$ . Although extended basis sets are known to be necessary for obtaining quantitative  $\gamma$  values for  $\pi$ -conjugated systems, we employ the standard 6–31G\* basis set except for Ni since this basis set is found to be sufficient to provide semiquantitative  $\gamma$  values for several hydrocarbon  $\pi$ -conjugated diradicaloids with intermediate and large diradical characters: the 6–31G\*+diffuse p ( $\zeta_p = 0.0523$ ) was shown to increase the  $\gamma$  value of a polycyclic diphenalenyl radical, IDPL, by only 10% as compared to that calculated by the 6–31G\* basis set at the Hartree-Fock (HF) level of approximation.<sup>11a</sup> For the Ni atom, the valence part of the SDD basis set was supplemented by one diffuse s ( $\zeta_s = 0.01$ ), one diffuse d ( $\zeta_d = 0.09$ ), and two diffuse p ( $\zeta_{p1} = 0.126499$  and  $\zeta_{p2} = 0.031784$ ) functions whereas the validity of the pseudopotential was assessed from comparison with all-electron calculations. This was achieved by carrying out UBHandHLYP  $\gamma$  calculations for compound 2 using Huzinaga's basis sets MIDI+p ( $\zeta_p = 0.088$ ), MIDI+pd ( $\zeta_{p,d} =$

**TABLE 1:**  $\gamma$  Values of **2** Calculated Using the MIDI+diff (diff = p, pd, and pdf) and SDD Basis Sets for Ni Atom

basis set for Ni	$\gamma^a$ [ $\times 10^3$ au]
MIDI+p	617
MIDI+pd	586
MIDI+pdf	595
SDD	612

<sup>a</sup> The  $\gamma$  values are calculated by the UBHandHLYP method using the 6-31G\* basis set for all atoms except for Ni.

0.088), and MIDI+pdf ( $\zeta_{p,d,f} = 0.088$ )<sup>26</sup> for Ni and 6-31G\* for other atoms. The results given in Table 1 demonstrate the good agreement between Huzinaga's basis sets and those using the SDD+6-31G\* basis set. For Se, we also employed the SDD basis set.

The  $\gamma$  values were calculated using the finite-field (FF) approach,<sup>27</sup> which consists of a fourth-order differentiation of the energy with respect to the applied external electric field. A power series expansion convention (called B convention<sup>28</sup>) was chosen for defining  $\gamma$ , and the following fourth-order numerical differentiation formula was employed:

$$\gamma = \frac{1}{36(F)^4} \{E(3F) - 12E(2F) + 39E(F) - 56E(0) + 39E(-F) - 12E(-2F) + E(-3F)\} \quad (3)$$

$E(F)$  indicates the total energy in the presence of the static electric field  $F$  in the  $x$ -direction. We used  $F$  values ranging from 0.0005 to 0.0050 au to obtain numerically stable  $\gamma$  values. Moreover, to achieve sufficiently accurate  $\gamma$  values, an ultrafine integration grid<sup>25</sup> and a tight convergence threshold of  $10^{-10}$  au on the energy were adopted. The  $\gamma$  values are given in atomic units (au): 1.0 au of  $\gamma$  is equal to  $6.235377 \times 10^{-65} \text{ C}^4 \text{ m}^4 \text{ J}^{-3}$  and  $5.0367 \times 10^{-40} \text{ esu}$ . All calculations were performed using the Gaussian 03 program package.<sup>25</sup>

We now briefly explain the  $\gamma$  density analysis,<sup>9,29</sup> which describes the spatial contribution of electrons to  $\gamma$ . This method is based on the expression

$$\gamma = -\frac{1}{3!} \int r \rho^{(3)}(\mathbf{r}) d^3r \quad (4)$$

where the third-order derivative of the electron density with respect to the electric field is given by

$$\rho^{(3)}(\mathbf{r}) = \left. \frac{\partial^3 \rho(\mathbf{r})}{\partial F^3} \right|_{F=0} \quad (5)$$

and is referred to as the  $\gamma$  density.<sup>9</sup> Positive and negative values of  $\rho^{(3)}(\mathbf{r})$  multiplied by  $F^3$  represent field-induced increase and decrease of the charge density, respectively, and are thus at the origin of the third-order dipole moment (third-order polarization) in the direction from positive to negative  $\gamma$  densities. The  $\gamma$  densities were calculated for a grid of points using a numerical third-order differentiation of the electron densities calculated by the Gaussian 03 program. The box dimensions ( $-10 \leq x \leq 10 \text{ \AA}$ ,  $-6 \leq y \leq 6 \text{ \AA}$ , and  $-5.0 \leq z \leq 5.0 \text{ \AA}$ ) ensure that the  $\gamma$  values obtained by integration are within 1% of the FF results. The relationship between  $\gamma$  and  $\rho^{(3)}(\mathbf{r})$  can be illustrated by considering the example of a pair of localized  $\gamma$  densities with positive and negative values: the sign of their contribution to the total  $\gamma$  is positive when the direction from positive to negative  $\gamma$  values coincides with the direction of the applied electric field and vice versa. Moreover, the magnitude of the contribution is proportional to the distance between two  $\gamma$  densities.

### 3. Results and Discussion

**3.1. Effects of the Donor Atom on the Diradical Character and the Orbitals.** Table 2 lists the  $\gamma$  values for complexes **1**–**7** calculated at the (U)BHandHLYP/SDD+6-31G\* level as well as the diradical characters (calculated from UNO/SDD+6-31G\* occupation numbers), the Mulliken electronegativities of the donor atoms, and the natural population analysis (NPA)<sup>30</sup> charges on the Ni and donor atoms calculated by the (U)BHandHLYP/SDD+6-31G\* method. The diradical characters of these complexes are found to vary from 0.0 to 0.884 upon changing the donor atoms. In this section, we discuss the cause of the variation in diradical characters.

Figure 2 shows the frontier UNOs corresponding to the unpaired electrons on both-end phenyl rings together with their occupation numbers for **1**–**5**. The increase of the diradical character is accompanied by an increase in the distribution of the frontier UNOs on both-end phenyl rings and the decrease of the distribution of these orbitals on the donor atoms in ligands. We also calculate the magnetic orbitals, which represent  $\alpha$  and  $\beta$  spin unpaired electrons for **1**–**5** at the UHF level of approximation (see Figure 3.) The magnetic orbitals for the  $\alpha$  spin electron are predominantly localized on one ligand, while those for the  $\beta$  spin electron are localized on the other ligand. The in- and out-of-phase mixing between the magnetic orbitals reproduces the main feature of the spatial distributions of the frontier UNOs. For complexes with larger diradical characters, the unpaired electrons are primarily distributed on both-end phenyl rings, whereas for complexes with smaller diradical character, the distributions at the donor atoms of the ligands are significantly enhanced. Moreover, the magnetic orbitals of the complexes with intermediate and small diradical characters are localized on one-side ligands but have tails on the opposite-side ligands, which allows the magnetic orbitals to overlap with each other and leads to a decrease of diradical character. Although the tail of **5** ( $y = 0.342$ ) is smaller than those of **3** and **4** ( $y = 0.595$  and  $y = 0.556$ , respectively), the smaller diradical character is attributed to the large overlap in the core region.

The tendency obtained from the frontier UNOs and magnetic orbitals coincides with that from the resonance structures (Figure 1): the diradical character of structure **II** with unpaired electrons on both-end phenyl rings is larger than that of structure **I** with unpaired electrons on the X donor atoms. On the basis of the resonance structures shown in Figure 1, it is predicted that the relative  $\pi$ -bond stability between C1–X (or C12–X) and C1–C6 (or C7–C12) determines the diradical characters of complexes. When the donor atoms tend to form strong  $\pi$ -bond with the phenyl-ring carbons, the contribution of structure **II** increases leading to an increase of the diradical character. Such an increase is generally associated with larger C1–C6/C7–C12 bond lengths (Figure S1).

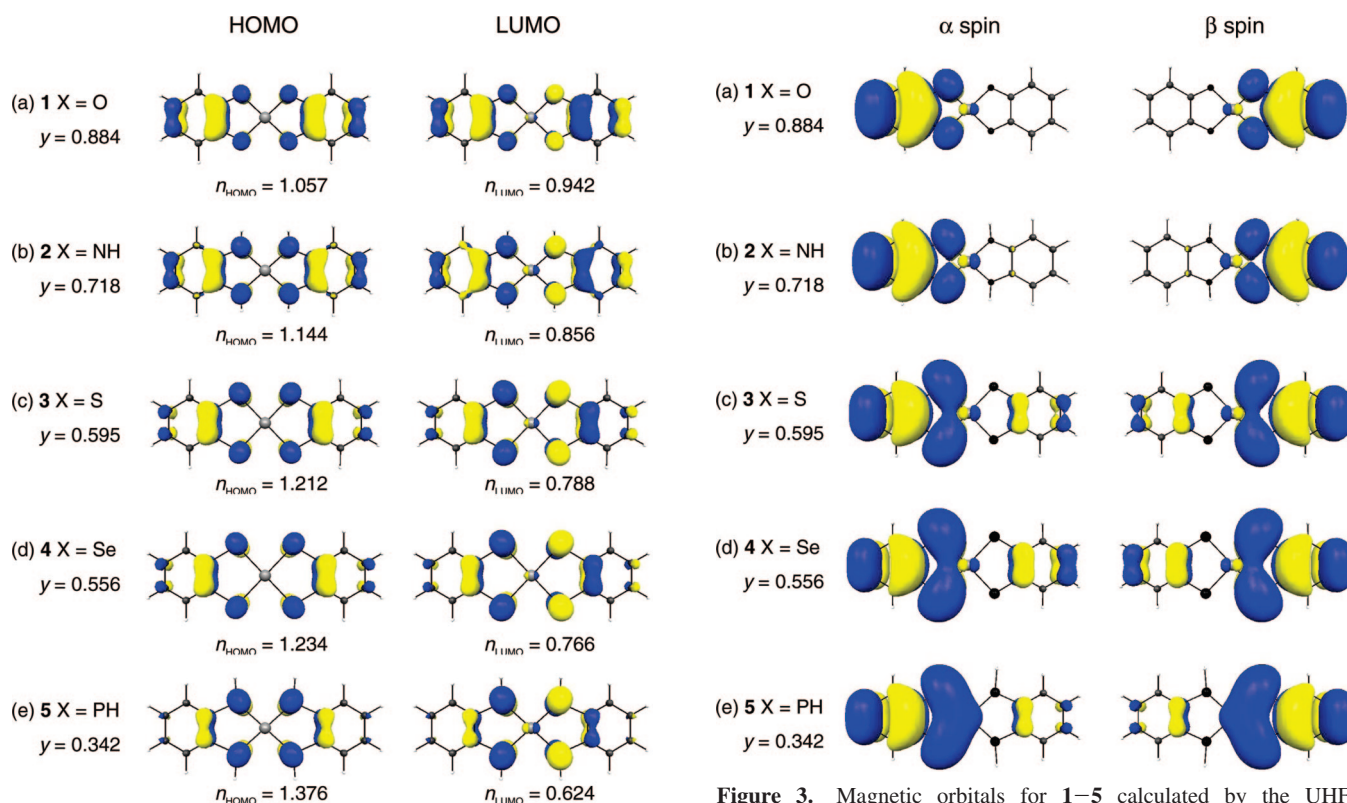
As seen from Table 2, the ability of the donor atom (X) to form  $\pi$ -bond with the phenyl-ring carbon atoms is related to the electronegativity of X. Donor atoms with large electronegativity possess low-lying HOMO (composed of outermost p orbital for O, N, S, Se, and P) that can form stable  $\pi$ -bonds with the phenyl-ring carbon atoms. It is therefore expected that the complexes involving donor atoms with larger electronegativities exhibit larger diradical characters. Indeed, the order of diradical characters for **1**–**5** is in good agreement with that of the X atom electronegativities (see Table 2). This suggests further that the diradical character of this type of complex can be controlled by adjusting the electronegativities of the donor atoms in the ligands.



**TABLE 2:**  $\gamma$  Values, Diradical Characters ( $y$ ), Mulliken Electronegativities  $\chi_M$  of Donor Atoms (X,Y), and NPA Charges on Ni and X(Y) for Complexes 1–7

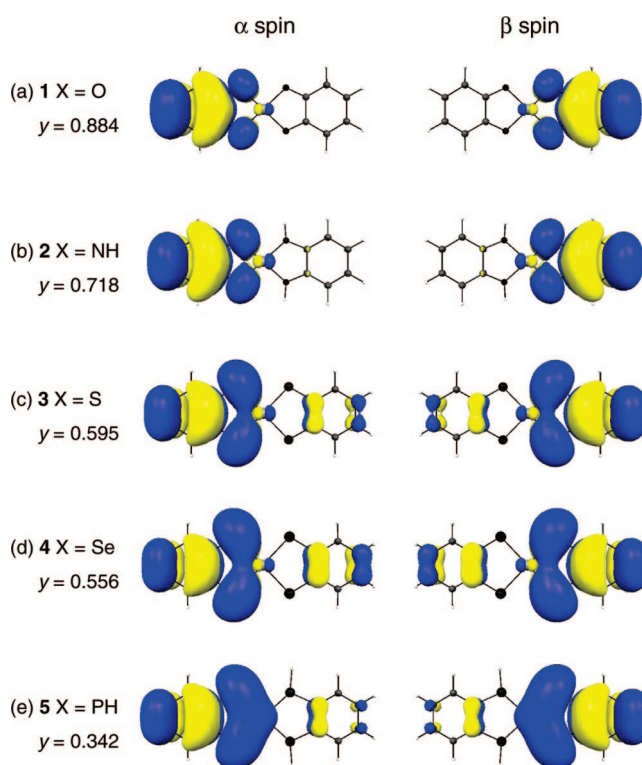
complex	O (1)	NH (2)	S (3)	Se (4)	PH (5)	NH, NH <sub>2</sub> (6)	S, NH <sub>2</sub> (7)
$y^a$ [–]	0.884	0.718	0.595	0.556	0.342	0.0	0.0
$\chi_M$ of X <sup>b</sup> [eV]	7.54	7.30	6.22	5.89	5.62	7.30	6.22
$\chi_M$ of Y <sup>b</sup> [eV]						7.30	7.30
charge on Ni <sup>c</sup>	1.268	1.103	0.631	0.499	0.448	1.101	0.893
charge on X <sup>d</sup>	–0.706	–0.432	–0.030	0.067	0.238	–0.639	–0.368
charge on Y <sup>d</sup>						–0.053	–0.031
$\gamma^e$ [ $\times 10^3$ au]	176	612	677	807	819	16	14

<sup>a</sup> The  $y$  values are calculated from UNO/SDD+6–31G\* occupation numbers. <sup>b</sup> Reference 32. <sup>c</sup> The NPA charges on Ni are calculated by the (U)BHandHLYP/SDD+6–31G\* method. <sup>d</sup> The NPA charges on the donor atoms X(Y) are calculated at the (U)BHandHLYP/SDD+6–31G level of approximation. For **2**, **5**, **6**, and **7**, the charges indicate the sum of charges on the donor atoms and hydrogens bonded with the donor atoms. <sup>e</sup> The  $\gamma$  values are calculated by the (U)BHandHLYP/SDD+6–31G\* method.

**Figure 2.** Frontier UNOs and their occupation numbers ( $n_{\text{HOMO}}$  and  $n_{\text{LUMO}}$ ) as well as diradical characters ( $y$ ) for **1–5** calculated by the UHF/SDD+6–31G\* method. The yellow and blue regions represent positive and negative NOs with contour values of  $\pm 0.05$  au, respectively.

The variations in diradical character of **1–5** are also accompanied by changes in the NPA charges on the central Ni atom and the donor atoms (see Table 2). When the diradical character increases, the positive NPA charge on Ni increases, while that on the donor atom decreases and then becomes negative for **1–3**. The diradical character was also evaluated in ref 15 for compounds similar to **1–3**. Though using either of their approximations the values are smaller or larger than ours, the largest diradical character was found for compound **1** and the smallest was found for compound **3**.

**3.2. Effects of the Donor Atom on  $\gamma$ .** The relationship between  $y$  and  $\gamma$  value is sketched in Figure 4 for **1–7** and follows the same structure–property relationship as in organic diradicals: the complexes with intermediate diradical characters (**3**, **4**, and **5**) exhibit larger  $\gamma$  values than that with large diradical character (**1**) and closed-shell complexes (**6** and **7**). The  $\gamma$  value of **5** ( $y = 0.342$  and  $\gamma = 819 \times 10^3$  au), which is the largest in

**Figure 3.** Magnetic orbitals for **1–5** calculated by the UHF/SDD+6–31G\* method. The yellow and blue regions represent contour values of  $\pm 0.02$  au, respectively.

these complexes, is found to be about 60 times larger than that of **7** ( $y = 0.0$  and  $\gamma = 14 \times 10^3$  au). This enhancement of  $\gamma$  suggests the advantage of diradical systems for third-order NLO properties of metal-involving systems.

The  $\gamma$  density distributions for **1–7** at the BHandHLYP/SDD+6–31G\* level of approximation are shown in Figure 5 in which spin-unrestricted and -restricted solutions are obtained for **1–5** and **6–7**, respectively. For all complexes, the primary positive contributions to  $\gamma$  come from  $\pi$ -electrons, while  $\sigma$ -electrons provide small negative contributions. For **1–5**, extended positive and negative  $\gamma$  densities are distributed well separately on the left- and right-hand side ligands, respectively, which leads to the dominant positive contributions to  $\gamma$ . Such distribution patterns are in good agreement with those of pure organic diradicals, for example, diphenalenyl diradical systems. For **1** with a large diradical character, the left- and right-hand side  $\gamma$  density distributions are significantly smaller than those of **2–5**. For closed-shell complexes **6** and **7**, the  $\gamma$  densities are negligible when adopting the same isocontour ( $\pm 200$  au). From the  $\gamma$  density maps of **6** and **7** (Figure 6) with a smaller contour

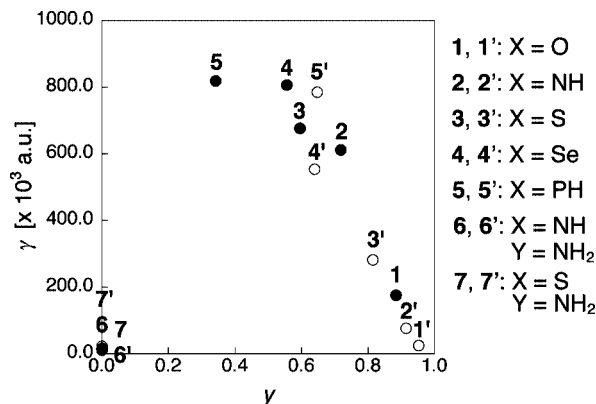


**Figure 4.** Diradical character ( $y$ ) dependence of  $\gamma$  [au] for original complexes **1–7** (●) and metal core eliminated complexes **1'–7'** (○).

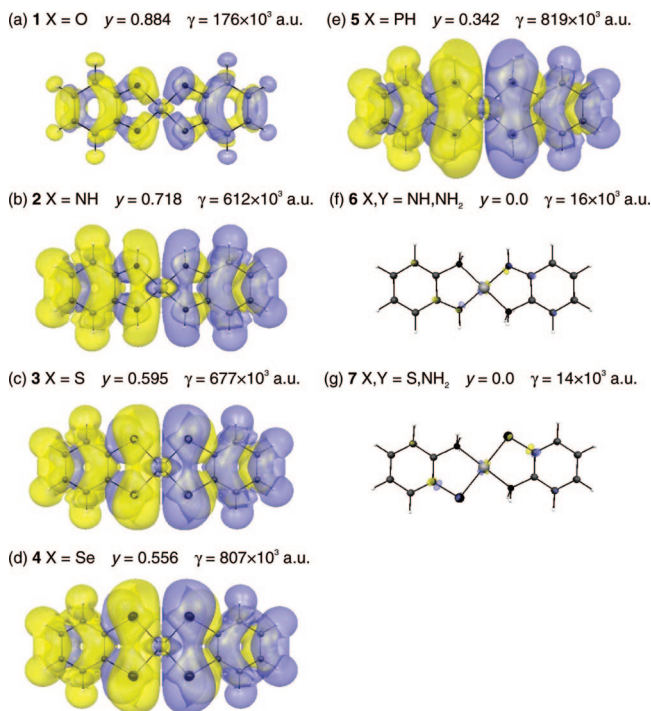
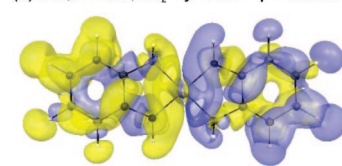


**Figure 5.**  $\gamma$  density distributions of **1–7** calculated at the (U)BHandHLYP/SDD+6-31G\* level of approximation. The yellow and blue meshes represent positive and negative  $\gamma$  densities with contour values of  $\pm 200$  au, respectively.

value ( $\pm 10$  au), positive and negative  $\gamma$  densities appear alternately along the bond pathway C7–Y–Ni–Y–C6 (C12–X–Ni–X–C1) and partly cancel each other. This pattern is also observed in conventional closed-shell polyenic systems.<sup>9</sup> These  $\gamma$  density distributions are found to well support the relative amplitudes of  $\gamma$  values for **1–7**.

Now, let us compare the  $\gamma$  and diradical character for **5** (which exhibits the largest  $\gamma$  value among the systems studied here) with those of pure organic diradical systems studied recently.<sup>10,11</sup> The  $\gamma$  value of **5** ( $y = 0.342$  and  $\gamma = 819 \times 10^3$  au) is about one-third of that of IDPL ( $y = 0.770$  and  $\gamma = 2284 \times 10^3$  au at the UBHandHLYP/6-31G\* level of approximation), which is a diradical compound exhibiting significantly large two-photon absorption.<sup>11c,31</sup> The difference can be attributed to the larger  $\pi$ -conjugation size in IDPL than in **5**. On the other hand, the  $\gamma$  value of **5** is about twice as large as that of BI2Y having a similar size to **5** ( $y = 0.423$  and  $\gamma = 484 \times 10^3$  au at the UBHandHLYP/6-31G level of approximation<sup>10c</sup>). This feature

(a) **6** X,Y = NH,NH<sub>2</sub>  $y = 0.0$   $\gamma = 16 \times 10^3$  a.u.



(b) **7** X,Y = S,NH<sub>2</sub>  $y = 0.0$   $\gamma = 14 \times 10^3$  a.u.

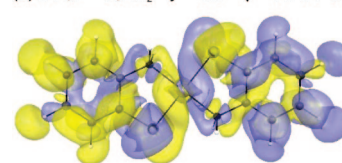


**Figure 6.**  $\gamma$  density distributions of **6** and **7** calculated by the RBHandHLYP/SDD+6-31G\* method. The yellow and blue meshes represent positive and negative  $\gamma$  densities with contour values of  $\pm 10$  au, respectively.

**TABLE 3:**  $\gamma$  Values for **1'–7'** Calculated by the (U)BHandHLYP/SDD+6-31G\* Method as well as the Diradical Characters

	NH (2')	S (3')	Se (4')	PH (5')	NH, NH <sub>2</sub> (6')	S, NH <sub>2</sub> (7')
compound	O (1')					
$y^a$ [–]	0.952	0.914	0.814	0.639	0.647	0.0
$\gamma$ [ $\times 10^3$ a.u.]	25	77	282	554	785	11

<sup>a</sup> The  $y$  values are calculated using the UNO/SDD+6-31G\* method.

suggests that, among diradical compounds and more particularly those presenting intermediate diradical character, the third-order NLO properties of transition-metal complexes could be larger than those of similar-size pure organic compounds.

**3.3. Effect of Central Nickel Atom on the Diradical Character and  $\gamma$ .** To reveal the effect of the central Ni atom on  $y$  and  $\gamma$ , we examined model systems without Ni<sup>2+</sup> core, that is, diradical compounds [(*o*-C<sub>6</sub>H<sub>4</sub>X<sub>2</sub>)<sub>2</sub>]<sup>2–</sup> [X = O (**1'**), NH (**2'**), S (**3'**), Se (**4'**), and PH (**5'**)] and closed-shell analogues [(*o*-C<sub>6</sub>H<sub>4</sub>XY)<sub>2</sub>]<sup>2–</sup> [(X, Y) = (NH, NH<sub>2</sub>) (**6'**) and (S, NH<sub>2</sub>) (**7'**)]. For **1'–7'**, we employed the geometries of the ligand parts as optimized geometries for **1–7**. The relationship between  $y$  and  $\gamma$  for **1'–7'** is shown in Figure 4 and Table 3. The elimination of Ni<sup>2+</sup> does not change the diradical character of the closed-shell **6** and **7** complexes, whereas it increases the diradical character for **1–5** though the degree of increase depends on the system. The increase in the diradical character of **1'–5'** is related to the amplitude of the negative charge increase on the ligands. Indeed, the order of the increase in the diradical character [ $\Delta y = y(n') - y(n)$ ] upon eliminating Ni<sup>2+</sup> is **1** ( $\Delta y = 0.068$ ) < **4** ( $\Delta y = 0.083$ ) < **2** ( $\Delta y = 0.196$ ) < **3** ( $\Delta y = 0.219$ ) < **5** ( $\Delta y = 0.305$ ) (see Figure 4), which follows the order of negative charge on the ligands, **1** > **2** > **3** > **4** > **5**, except for **4**. Moreover, the relationship between  $y$  and  $\gamma$  for **1'–7'** is in good agreement with that for **1–7** (see Figure 4). Namely, although the metal core does not directly contribute to the  $\gamma$  values as shown in the  $\gamma$  density distributions (Figure 5), it modulates  $\gamma$  through the change in the diradical character associated with its charge. Thus, in addition to the role of the ligand atoms, the diradical character and second hyperpolarizability of these complexes are tunable as a function of the metal core species.

#### 4. Summary

Using the UBHandHLYP method, we have theoretically investigated the diradical character dependence of  $\gamma$  in square



planar complexes of Ni with bidentate ligands (*o*-C<sub>6</sub>H<sub>4</sub>XY). Upon modifying the X donor atoms of the ligands, the diradical character of these complexes changes strongly: the larger the X electronegativities, the larger the diradical character. This relationship can be understood by the relative contributions of the resonance structures **I** and **II** shown in Figure 1: a large electronegativity of X increases the contribution of **II** leading to a large diradical character. Along with the variation of diradical character from 0.0 to 0.884 by modifying the donor atoms X, the  $\gamma$  values change substantially from  $14 \times 10^3$  to  $819 \times 10^3$  au. These results indicate that the structure–property relationship deduced from pure organic diradical systems is also applicable to these metal-involving complexes, whose diradical characters and  $\gamma$  values can be controlled by modifying donor atoms X in the ligands. Furthermore, the results of eliminating the Ni<sup>2+</sup> core suggest that a modification of the metal core also affects the diradical character and  $\gamma$  values of this type of complexes. Unfortunately, the calculated  $\gamma$  values cannot be compared to the experimental results because the latter have been recorded in resonance conditions. Nevertheless, they provide a fundamental understanding of third-order NLO properties of these complexes to stimulate new third-order NLO measurements on these or related systems.

These complexes present also several advantages including (1) their facile synthesis in comparison with diradical systems like the diphenalenyl species, (2) the control of  $\gamma$  by chemical modification of the ligands or the metal, (3) the possibility to prepare metal-coordinated polymers with multiradical characters, which have been predicted to exhibit further enhancement of  $\gamma$ ,<sup>33</sup> and (4) the use of ligands as molecular switches of which the two-photon fluorescence or other NLO responses would change upon metal recognition and complexation in the same spirit as recent studies on molecular switches exhibiting large variations of NLO responses when tuning the pH, the redox potential, or irradiating with photons.<sup>34</sup> To further confirm these features, the investigation on this type of complex with different metal cores as well as on more extended species involving multimetal cores is in progress in our laboratory.

**Acknowledgment.** This work is supported by Grant-in-Aid for Scientific Research (Nos. 18350007 and 20655003) from Japan Society for the Promotion of Science (JSPS), Grant-in-Aid for Scientific Research on Priority Areas (No. 18066010) from the Ministry of Education, Science, Sports, and Culture of Japan, and the global COE (center of excellence) program Global Education and Research Center for Bio-Environmental Chemistry of Osaka University. E.B. thanks the IUAP program N° P6-27 for her postdoctoral grant. B.C. thanks the Fund for Scientific Research (FRS-FNRS) for his Research Director position.

**Supporting Information Available:** Bond lengths for **1**–**7** optimized at the (U)B3LYP/SDD+6–31G\* level of approximation. This material is available free of charge via the Internet at <http://pubs.acs.org>.

## References and Notes

- Pathenopoulos, D. A.; Rentzepis, P. M. *Science* **1989**, *245*, 893.
- Zhou, W.; Kuebler, S. M.; Braun, K. L.; Yu, T.; Cammack, J. K.; Ober, C. K.; Perry, J. W.; Marder, S. R. *Science* **2002**, *296*, 1106.
- Frederiksen, P. K.; Jørgensen, M.; Ogilby, P. R. *J. Am. Chem. Soc.* **2001**, *123*, 1215.
- Kaiser, W.; Garrett, C. G. B. *Phys. Rev. Lett.* **1961**, *7*, 229.
- Heflin, J. R.; Wong, K. Y.; Zamani-Khamiri, O.; Garito, A. F. *Phys. Rev. B* **1988**, *38*, 1573.
- (a) Beljonne, D.; Shuai, Z.; Brédas, J. L. *J. Chem. Phys.* **1993**, *98*, 8819. (b) Tykwinski, R. R.; Gubler, U.; Martin, R. E.; Diederich, F.; Bosshard, C.; Günter, P. *J. Phys. Chem. B* **1998**, *102*, 4451. (c) Toto, J. L.; Toto, T. T.; de Melo, C. P.; Kirtman, B.; Robins, K. *J. Chem. Phys.* **1996**, *104*, 8586. (d) Tretiak, S.; Chernyak, V.; Mukamel, S. *Phys. Rev. Lett.* **2006**, *77*, 4656.
- (a) Nakano, M.; Yamaguchi, K.; Fueno, T. *Chem. Phys. Lett.* **1991**, *185*, 550. (b) Meyers, F.; Marder, S. R.; Pierce, B. M.; Brédas, J. L. *J. Am. Chem. Soc.* **1994**, *116*, 10703. (c) Ferrighi, L.; Frediani, L.; Cappelli, C.; Salek, P.; Ågren, H.; Helgaker, T.; Ruud, K. *Chem. Phys. Lett.* **2006**, *425*, 267.
- (a) Nakano, M.; Fujita, H.; Takahata, M.; Yamaguchi, K. *J. Am. Chem. Soc.* **2002**, *124*, 9648. (b) Bulat, F. A.; Toro-Labbé, A.; Champagne, B.; Kirtman, B.; Yang, W. *J. Chem. Phys.* **2005**, *123*, 014319.
- (a) de Melo, C. P.; Silbey, R. J. *J. Chem. Phys.* **1988**, *88*, 2567. (b) Villesuzanne, A.; Hoarau, J.; Ducasse, L.; Olmedo, L.; Hourquebie, P. *J. Chem. Phys.* **1992**, *96*, 495. (c) Nakano, M.; Shigemoto, I.; Yamada, S.; Yamaguchi, K. *J. Chem. Phys.* **1995**, *103*, 4175. (d) Champagne, B.; Spassova, M.; Jadin, J. B.; Kirtman, B. *J. Chem. Phys.* **2002**, *116*, 3935. (e) Oliveira, L. N.; Amaral, O. A. V.; Castro, M. A.; Fonseca, T. L. *Chem. Phys.* **2003**, *289*, 221.
- (a) Nakano, M.; Kishi, R.; Nitta, T.; Kubo, T.; Nakasuji, K.; Kamada, K.; Ohta, K.; Champagne, B.; Botek, E.; Yamaguchi, K. *J. Phys. Chem. A* **2005**, *109*, 885. (b) Nakano, M.; Kishi, R.; Ohta, S.; Takebe, A.; Takahashi, H.; Furukawa, S.; Kubo, T.; Morita, Y.; Nakasuji, K.; Yamaguchi, K.; Kamada, K.; Ohta, K.; Champagne, B.; Botek, E. *J. Chem. Phys.* **2006**, *125*, 74113. (c) Nakano, M.; Kishi, R.; Nakagawa, N.; Ohta, S.; Takahashi, H.; Furukawa, S.; Kamada, K.; Ohta, K.; Champagne, B.; Botek, E.; Yamada, S.; Yamaguchi, K. *J. Phys. Chem. A* **2006**, *110*, 4238. (d) Ohta, S.; Nakano, M.; Kubo, T.; Kamada, K.; Ohta, K.; Kishi, R.; Nakagawa, N.; Champagne, B.; Botek, E.; Takebe, A.; Umezaki, S.; Nate, M.; Takahashi, H.; Furukawa, S.; Morita, Y.; Nakasuji, K.; Yamaguchi, K. *J. Phys. Chem. A* **2007**, *111*, 3633. (e) Nakano, M.; Nagao, H.; Yamaguchi, K. *Phys. Rev. A* **1997**, *55*, 1503.
- (a) Nakano, M.; Kubo, T.; Kamada, K.; Ohta, K.; Kishi, R.; Ohta, S.; Nakagawa, N.; Takahashi, H.; Furukawa, S.; Morita, Y.; Nakasuji, K.; Yamaguchi, K. *Chem. Phys. Lett.* **2006**, *418*, 142. (b) Ohta, S.; Nakano, M.; Kubo, T.; Kamada, K.; Ohta, K.; Kishi, R.; Nakagawa, N.; Champagne, B.; Botek, E.; Umezaki, S.; Takebe, A.; Takahashi, H.; Furukawa, S.; Morita, Y.; Nakasuji, K.; Yamaguchi, K. *Chem. Phys. Lett.* **2006**, *420*, 432. (c) Nakano, M.; Nakagawa, N.; Ohta, S.; Kishi, R.; Kubo, T.; Kamada, K.; Ohta, K.; Champagne, B.; Botek, E.; Takahashi, H.; Furukawa, S.; Morita, Y.; Nakasuji, K.; Yamaguchi, K. *Chem. Phys. Lett.* **2006**, *429*, 174. (d) Nakano, M.; Nakagawa, N.; Kishi, R.; Ohta, S.; Nate, M.; Takahashi, H.; Kubo, T.; Kamada, K.; Ohta, K.; Champagne, B.; Botek, E.; Morita, Y.; Nakasuji, K.; Yamaguchi, K. *J. Phys. Chem. A* **2007**, *111*, 9102.
- (a) Champagne, B.; Botek, E.; Nakano, M.; Nitta, T.; Yamaguchi, K. *J. Chem. Phys.* **2005**, *122*, 114315. (b) Champagne, B.; Botek, E.; Quinet, O.; Nakano, M.; Kishi, R.; Nitta, T.; Yamaguchi, K. *Chem. Phys. Lett.* **2005**, *407*, 372.
- (a) Nakano, M.; Kishi, R.; Ohta, S.; Takahashi, H.; Kubo, T.; Kamada, K.; Ohta, K.; Botek, E.; Champagne, B. *Phys. Rev. Lett.* **2007**, *99*, 033001-1.
- (a) Nakano, M.; Kishi, R.; Nakagawa, N.; Nitta, T.; Kubo, T.; Nakasuji, K.; Kamada, K.; Ohta, K.; Champagne, B.; Botek, E.; Yamaguchi, K. *J. Nonlinear Opt., Quantum Opt.* **2005**, *34*, 29.
- Bachler, V.; Olbrich, G.; Neese, F.; Wieghardt, K. *Inorg. Chem.* **2002**, *41*, 4179.
- Ray, K.; Weyhermüller, T.; Neese, F.; Wieghardt, K. *Inorg. Chem.* **2005**, *44*, 5345.
- (a) Kafafi, Z. H.; Lindle, J. R.; Weisbecker, C. S.; Bartoli, F. J.; Shirk, J. S.; Yoon, T. H.; Kim, O. K. *Chem. Phys. Lett.* **1991**, *179*, 79. (b) Kafafi, Z. H.; Lindle, J. R.; Flom, S. R.; Pong, R. G. S.; Weisbecker, C. S.; Claussen, R. C.; Bartoli, F. J. *Proc. SPIE* **1992**, *1626*, 440. (c) Dhindsa, A. S.; Underhill, A. E.; Oliver, S. N.; Kershaw, S. V. *Nonlinear Opt.* **1995**, *10*, 115. (d) Dhindsa, A. S.; Underhill, A. E.; Oliver, S. N.; Kershaw, S. V. *Proc. SPIE* **1995**, *2531*, 350.
- Lauterbach, C.; Fabian, J. *Eur. J. Inorg. Chem.* **1999**, 1999, 1995.
- Kubo, T.; Shimizu, A.; Uruichi, M.; Yakushi, K.; Nakano, M.; Shiomi, D.; Sato, K.; Takui, T.; Morita, Y.; Nakasuji, K. *Org. Lett.* **2007**, *9*, 81.
- Dolg, M.; Wedig, U.; Stoll, H.; Preuss, H. *J. Chem. Phys.* **1987**, *86*, 866.
- Bergner, A.; Dolg, M.; Küchle, W.; Stoll, H.; Preuß, H. *Mol. Phys.* **1993**, *80*, 1431.
- Yamaguchi, K. *Self-Consistent Field: Theory and Applications*; Carbo, R., Klobukowski, M., Eds.; Elsevier: Amsterdam, 1990; p 727.
- Yamanaka, S.; Okumura, M.; Nakano, M.; Yamaguchi, K. *J. Mol. Struct. (THEOCHEM)* **1994**, *310*, 205.
- Herebian, D.; Wieghardt, K. E.; Neese, F. *J. Am. Chem. Soc.* **2003**, *125*, 10997.
- Frisch, M. J.; Trucks, G. W.; Schlegel, H. B.; Scuseria, G. E.; Robb, M. A.; Cheeseman, J. R.; Montgomery, J. A., Jr.; Vreven, T.; Kudin, K. N.;

Burant, J. C.; Millam, J. M.; Iyengar, S. S.; Tomasi, J.; Barone, V.; Mennucci, B.; Cossi, M.; Scalmani, G.; Rega, N.; Petersson, G. A.; Nakatsuji, H.; Hada, M.; Ehara, M.; Toyota, K.; Fukuda, R.; Hasegawa, J.; Ishida, M.; Nakajima, T.; Honda, Y.; Kitao, O.; Nakai, H.; Klene, M.; Li, X.; Knox, J. E.; Hratchian, H. P.; Cross, J. B.; Bakken, V.; Adamo, C.; Jaramillo, J.; Gomperts, R.; Stratmann, R. E.; Yazyev, O.; Austin, A. J.; Cammi, R.; Pomelli, C.; Ochterski, J. W.; Ayala, P. Y.; Morokuma, K.; Voth, G. A.; Salvador, P.; Dannenberg, J. J.; Zakrzewski, V. G.; Dapprich, S.; Daniels, A. D.; Strain, M. C.; Farkas, O.; Malick, D. K.; Rabuck, A. D.; Raghavachari, K.; Foresman, J. B.; Ortiz, J. V.; Cui, Q.; Baboul, A. G.; Clifford, S.; Cioslowski, J.; Stefanov, B. B.; Liu, G.; Liashenko, A.; Piskorz, P.; Komaromi, I.; Martin, R. L.; Fox, D. J.; Keith, T.; Al-Laham, M. A.; Peng, C. Y.; Nanayakkara, A.; Challacombe, M.; Gill, P. M. W.; Johnson, B.; Chen, W.; Wong, M. W.; Gonzalez, C.; Pople, J. A. *Gaussian 03*, revision C.02; Gaussian, Inc.: Wallingford, CT, 2004.

(26) Huzinaga, S.; Andzelm, J.; Klobukowski, M.; Radzio-Andzelm, E.; Sakai, Y.; Tatewaki, H. *Gaussian Basis Sets for Molecular Calculations*; Elsevier: Amsterdam, 1984.

(27) Cohen, H. D.; Roothaan, C. C. J. *J. Chem. Phys.* **1965**, *43*, S34.

(28) Willetts, A.; Rice, J. E.; Burland, D. M.; Shelton, D. P. *J. Chem. Phys.* **1992**, *97*, 7590.

(29) (a) Nakano, M.; Yamaguchi, K.; Fueno, T. *Chem. Phys. Lett.* **1991**, *185*, 550. (b) Nakano, M.; Yamada, S.; Shigemoto, I.; Yamaguchi, K. *Chem.*

*Phys. Lett.* **1996**, *250*, 247. (c) Nakano, M.; Fujita, H.; Takahata, M.; Yamaguchi, K. *Chem. Phys. Lett.* **2002**, *356*, 462.

(30) (a) Reed, A. E.; Weinhold, F. *J. Chem. Phys.* **1983**, *78*, 4066. (b) Reed, A. E.; Weinstock, R. B.; Weinhold, F. *J. Chem. Phys.* **1985**, *83*, 735. (c) Reed, A. E.; Curtiss, L. A.; Weinhold, F. *Chem. Rev.* **1988**, *88*, 899.

(31) Kamada, K.; Ohta, K.; Kubo, T.; Shimizu, A.; Morita, Y.; Nakasuji, K.; Kishi, R.; Ohta, S.; Furukawa, S.; Takahashi, H.; Nakano, M. *Angew. Chem., Int. Ed.* **2007**, *46*, 3544.

(32) Pearson, R. G. *Inorg. Chem.* **1988**, *27*, 734.

(33) Nakano, M.; Takebe, A.; Kishi, R.; Ohta, S.; Nate, M.; Kubo, T.; Kamada, K.; Ohta, K.; Champagne, B.; Botek, E.; Takahashi, H.; Furukawa, S.; Morita, Y.; Nakasuji, K. *Chem. Phys. Lett.* **2006**, *432*, 473.

(34) (a) Coe, B. J.; Harris, J. A.; Jones, L. A.; Brunschwig, B. S.; Song, K.; Clays, K.; Garin, J.; Orduna, J.; Coles, S. J.; Hursthouse, M. B. *J. Am. Chem. Soc.* **2005**, *127*, 4845. (b) Sanguinet, L.; Pozzo, J.-L.; Rodriguez, V.; Adamietz, F.; Castet, F.; Ducasse, L.; Champagne, B. *J. Phys. Chem. B* **2005**, *109*, 11139. (c) Plaquet, A.; Guillaume, M.; Champagne, B.; Rougier, L.; Mançois, F.; Rodriguez, V.; Pozzo, J.-L.; Ducasse, L.; Castet, F. *J. Phys. Chem. C* **2008**, *112*, 5638.

JP804400S